



## Green Synthesis, Characterization and Investigating the Antibacterial Potential of Silver Nanoparticles Using *Datura innoxia* (Datura innoxia) Against Bovine Mastitis Causing Bacteria

Journal:	Science Progress
Manuscript ID	SCI-25-1476
Manuscript Type:	Original Research Article
Date Submitted by the Author:	02-Jul-2025
Complete List of Authors:	qadeer, Saima; University of Education Ashraf, Asma; University of Education Bibi, Fozia; University of Education, Department of Zoology Asad, Muhammad; University of Education
Keywords:	Bovine Mastitis, AgNPs, Datura innoxia,, Green Synthesis, nanoparticles
Abstract:	<p><b>Objective:</b> The objective of this study was to biosynthesize the AgNPs from the aqueous leaf extract of the <i>D. innoxia</i>, characterize them and to evaluate their antibacterial potential against the bacteria associated with bovine mastitis.</p> <p><b>Methods:</b> The AgNPs were synthesized, purified, optimized and characterized using UV-Vis, XRD, SEM, TEM, HR-TEM and FTIR. Further, In vitro antibacterial activity of the different concentrations of synthesized AgNPs (5, 10, 15, and 20 mg/mL) was assessed against bacterial isolates cultured from milk samples of affected buffaloes, bacteria were identified using standard microbiological techniques.</p> <p><b>Results:</b> The synthesized AgNPs exhibited a characteristic surface plasmon resonance peak at 330-350 nm, while XRD analysis showed the intense diffraction peaks at <math>2\theta</math> angles of <math>33^\circ</math>, <math>46^\circ</math>, and <math>58^\circ</math>, within the range of <math>17^\circ</math> and <math>65^\circ</math>. SEM reveals polydisperse, irregular shaped nanoparticles clusters, further confirmed by TEM as aggregates of nearly spherical to slightly rod-shaped units (20-30nm), consistent with the 24-25 nm crystallite size from XRD and verified by HRTEM. FTIR analysis identify the capping agents that reduce and stabilize the AgNPs. Identified bacterial genera included <i>Staphylococcus</i> spp., <i>Streptococcus</i> spp., <i>Enterococcus</i> spp., <i>Corynebacterium</i> spp. (Gram-positive), <i>E. coli</i>, <i>Klebsiella</i> spp., <i>P. aeruginosa</i>, and <i>Enterobacter</i> spp. (Gram-negative). The AgNPs exhibited antibacterial activity in the agar well diffusion assay, with the largest zone of inhibition (<math>18.3 \pm 0.2</math>mm) observed against <i>Staphylococcus</i> at 20 mg/mL of AgNPs. The maximum antibacterial activity of AgNPs was observed at a MIC of 10 <math>\mu</math>L, particularly against <i>Staphylococcus</i> species.</p> <p><b>Conclusion:</b> These finding suggest that AgNPs synthesized from <i>D. innoxia</i> have strong antibacterial activity against mastitis-associated pathogens.</p>

1  
2  
3  
4  
5  
6  
7  
8  
9  
10  
11  
12  
13  
14  
15  
16  
17  
18  
19  
20  
21  
22  
23  
24  
25  
26  
27  
28  
29  
30  
31  
32  
33  
34  
35  
36  
37  
38  
39  
40  
41  
42  
43  
44  
45  
46  
47  
48  
49  
50  
51  
52  
53  
54  
55  
56  
57  
58  
59  
60



**Green Synthesis, Characterization and Investigating the Antibacterial Potential of Silver Nanoparticles Using Datura (*Datura innoxia*) Against Bovine Mastitis Causing Bacteria**

Saima Qadeer,<sup>1\*</sup> Asma Ashraf<sup>1</sup>, Fouzia Bibi<sup>1</sup>, Muhammad Asad<sup>1</sup>

<sup>1</sup> *Department of Zoology, Division of Sciences and Technology, University of Education, Lahore-54000 Pakistan*

---

\*Corresponding Author:

Dr. Saima Qadeer

[saima.qadeer@ue.edu.pk](mailto:saima.qadeer@ue.edu.pk)

1  
2  
3  
4  
5  
6  
7  
8  
9  
10  
11  
12  
13  
14  
15  
16  
17  
18  
19  
20  
21  
22  
23  
24  
25  
26  
27  
28  
29  
30  
31  
32  
33  
34  
35  
36  
37  
38  
39  
40  
41  
42  
43  
44  
45  
46  
47  
48  
49  
50  
51  
52  
53  
54  
55  
56  
57  
58  
59  
60

**Abstract:**

**Objective:** The objective of this study was to biosynthesize the AgNPs from the aqueous leaf extract of the *D. inoxia*, characterize them and to evaluate their antibacterial potential against the bacteria associated with bovine mastitis.

**Methods:** The AgNPs were synthesized, purified, optimized and characterized using UV-Vis, XRD, SEM, TEM, HR-TEM and FTIR. Further, In vitro antibacterial activity of the different concentrations of synthesized AgNPs (5, 10, 15, and 20 mg/mL) was assessed against bacterial isolates cultured from milk samples of affected buffaloes, bacteria were identified using standard microbiological techniques.

**Results:** The synthesized AgNPs exhibited a characteristic surface plasmon resonance peak at 330-350 nm, while XRD analysis showed the intense diffraction peaks at  $2\theta$  angles of  $33^\circ$ ,  $46^\circ$ , and  $58^\circ$ , within the range of  $17^\circ$  and  $65^\circ$ . SEM reveals polydisperse, irregular shaped nanoparticles clusters, further confirmed by TEM as aggregates of nearly spherical to slightly rod-shaped units (20-30nm), consistent with the 24-25 nm crystallite size from XRD and verified by HRTEM. FTIR analysis identify the capping agents that reduce and stabilize the AgNPs. Identified bacterial genera included *Staphylococcus spp.*, *Streptococcus spp.*, *Enterococcus spp.*, *Corynebacterium spp.* (Gram-positive), *E. coli*, *Klebsiella spp.*, *P. aeruginosa*, and *Enterobacter spp.* (Gram-negative). The AgNPs exhibited antibacterial activity in the agar well diffusion assay, with the largest zone of inhibition ( $18.3\pm0.2\text{mm}$ ) observed against *Staphylococcus* at 20 mg/mL of AgNPs. The maximum antibacterial activity of AgNPs was observed at a MIC of 10  $\mu\text{L}$ , particularly against *Staphylococcus* species.

**Conclusion:** These finding suggest that AgNPs synthesized from *D. inoxia* have strong antibacterial activity against mastitis-associated pathogens.

**Keywords:** Bovine Mastitis, AgNPs, *Datura innoxia*, Green Synthesis, nanoparticles

## 1. Introduction

Mastitis in buffalo is a painful inflammation of the udder tissues. It is considered as the highly widespread disease causing economic losses in the dairy sector due to decreased milk production and poor quality <sup>1</sup>. Bacteria are primarily responsible for about 70% of cases involved in the etiology of mastitis, the remaining 30% attributed to other agents such as mechanical or physical injury to the gland, etc. <sup>2</sup>. Major bacterial agents that cause mastitis include environmental (*Streptococcus agalactiae*, *E. coli*, *Enterobacter*, and *Klebsiella*) and infectious (*Staphylococcus aureus* and *Corynebacterium bovis*) <sup>3, 4</sup>. The most common method for treating and preventing mastitis is the use of antimicrobial agents, however, misuse has increased the antibiotic resistance <sup>5</sup>. The persistence of enterotoxins in milk and milk products, along with the possibility of pathogen transmission, makes it potentially dangerous to human health <sup>6</sup>. Due to its complex pathophysiology and emerging resistance, mastitis is sometimes extremely difficult to treat with traditional medications <sup>2</sup>.

To reduce the need for antibiotics in mastitis treatment, researchers have explored new therapeutic strategies. The realization that a substance's size could affect its physicochemical properties, highlighted the therapeutic potential of nanoparticles <sup>7</sup>. The green synthesized antibacterial nanoparticles have emerged as crucial tools against antibiotic resistant bacteria <sup>8</sup>. One of the most widely used nanoparticles is silver nanoparticles (AgNPs) <sup>9</sup>, because microorganisms are unable to develop resistance silver, which target multiple sites within the pathogen <sup>10</sup>. Because of their large surface area to volume ratio, silver nanoparticles possess enhanced antimicrobial potential <sup>11</sup>. AgNPs are widely used to treat microbial diseases because of their strong antiviral, antifungal, and antibacterial properties as well as their antioxidant

1  
2  
3  
4  
5  
6  
7  
8  
9  
10  
11  
12  
13  
14  
15  
16  
17  
18  
19  
20  
21  
22  
23  
24  
25  
26  
27  
28  
29  
30  
31  
32  
33  
34  
35  
36  
37  
38  
39  
40  
41  
42  
43  
44  
45  
46  
47  
48  
49  
50  
51  
52  
53  
54  
55  
56  
57  
58  
59  
60

activity. Intriguingly, most studies report no evidence of toxicity or accumulation in critical organs after topical AgNPs treatment. In order to improve AgNPs' biocompatibility and further reduce their toxicity often associated with chemical reducing agent during preparation used in conventional synthesis, green biosynthesis has recently been adopted <sup>12</sup>. AgNPs have numerous uses in the medical sphere, including gene therapy, wounds and burn coverings, dental coatings, and drug transport to specific tissues. In industrial sector, they are used in the production of textiles and cosmetics <sup>13</sup>. AgNPs kill bacteria through three ways; (I) leaching of metal ions that directly interact with bacterial cell and cause toxicity <sup>14</sup>, (II) stimulate the production of ROS in bacterial cells, oxidative stress results in animal death <sup>15</sup>, and (III) disruption of cell membrane permeability that leads to animal death <sup>16</sup>. The green synthesis using plant extract has been found to provide additional pharmacological properties to AgNPs <sup>17</sup>. Although numerous plant extracts have been used to synthesize the nanomaterials, the field remain active because diverse species can perform as capping and reducing agents, yielding nanoparticles with unique structures and properties <sup>18</sup>. Polyphenols and proteins found in plant extract can perform as reducing and capping resources, lowering the valence state of metal ions and giving a precise and stable form to AgNPs <sup>19, 20</sup>.

*Datura (D. inoxia)*, a shrubby plant from the Solanaceae family, generally recognized as thorn-apple and devil's trumpet, has shown remarkable antioxidant activity<sup>21</sup>. It is reported that seed extracts from various *Datura* species effectively scavenge free radicals and neutralize the stable diphenylpicrylhydrazyl (DPPH) <sup>22</sup>. It has been documented that this plant is cytotoxic to several cancer cells, and has been utilized in traditional medicine to treat a variety of conditions, such as cutaneous eruptions, colds, and neurological illnesses <sup>23</sup>. According to <sup>24</sup>, an ethanolic extract of *D. inoxia* shown antiproliferation properties against a range of cancer cells. Specifically extract

effectively inhibits the development of the cancer cells by causing death. Research suggested that, *D. inoxia* triggers apoptosis by raising the SubG1 phase and inducing an increase of apoptotic cells. Elevated e markers in LoVo cells further confirm that *D. inoxia* initiate apoptosis. Aqueous leaf extract of *D. inoxia* suppresses K562 cell proliferation in a dose and time-dependent manner, according to the results of cytotoxicity assay. Additionally, normal human B lymphoid cells were less susceptible to *D. inoxia*'s cytotoxicity than K562 cells <sup>25</sup>. Furthermore, *D. inoxia* has been documented to have many medical uses, including the treatment of respiratory conditions, soothing antispasmodics, and alleviating pain <sup>26</sup>. Additional phytochemicals existing in the plant, like flavonoids, phenols, saponins and glycosides, have been shown to have pain reliever, antibacterial, antipyretic, and anti-inflammatory properties <sup>27</sup>, <sup>28</sup>. Therefore, it was hypothesized that the biological action of AgNPs can be enhanced by combining them with *Datura* (*D. inoxia*) leaf extract. The objective of the current study is green synthesis of AgNPs from *D. inoxia*, their characterization and assessment of their antimicrobial action against mastitis causing bacterial.

## 2. Materials and Methods

### 2.1. The AgNPs Synthesis:

The plant species *Datura inoxia*, was identified according to Flora of Pakistan (Taxon Id:109368). Fresh leaves were collected, washed, dried, and ground into a fine powder, and extract was prepared according to <sup>29</sup> and stored at 4°C. Leaf extract was used to reduce AgNO<sub>3</sub> solution (1mM) into AgNPs <sup>30</sup>. The solution was heated at 70 °C for 1h <sup>29</sup>, resulting solution became dark brown, indicating the formation of AgNPs. The approach of <sup>31</sup> was used for the purification of AgNPs by diluting them in distilled water and centrifuging (Model Z216MK) them for 5 min at 12,000 rpm.

**2.2. AgNPs Characterization:** A UV visible spectroscopy machine (LX210DS) used to measure the visual properties of AgNPs within 200–800 nm range. For morphological assessment, AgNPs were examined under a scanning electron microscope (Cube II Emcraft, South Korea). TEM and HRTEM analysis were carried out on JEOL JEM-ARM200F. Metallurgical crystal-like characteristics of AgNPs were evaluated by X-ray diffraction machine (JDX-11, Joel Ltd., Japan) and obtained data were analyzed using software Origin Pro version 9.0. The size of nanoparticles was calculated by applying the Scherrer equation:  $d = \frac{k\lambda}{B \cos \theta}$  ),  $\lambda$ = X-ray wavelength, ( $d$ =Mean size,  $k$  = Dimensionless shape element (Value 0.9),  $\beta$ = Line broadening at half the maximum intensity,  $\theta$ = Bragg angle). Functional groups were identified by FTIR analysis (Nicolet, Summit LITE, Thermo-Scientific).

**2.3. Bacteria Culturing:**

Milk sample from Twelve mastitis affected Nili Ravi buffaloes was collected at the Livestock Diagnostic Laboratory, Khushab. The bacteria were separated by serial dilution according to <sup>32</sup>, cultured on nutrient agar according to <sup>33</sup>. Pure cultures were obtained from mixed cultures using the plate streaking method by <sup>34</sup>.

**2.4. Identification of Bacterial Genera:**

Simple staining was performed to determine the form and structure of bacteria, using common stains according to method by <sup>35</sup>. Gram Staining, which distinguishes bacteria according to the structure of their cell walls was carried out to identify unknown bacteria, given by <sup>36</sup>. Motility test was used to investigate the movement of living bacteria according to method given by <sup>37</sup>. Catalase test was used to find the catalase enzyme in bacteria according to method given by <sup>38</sup>.

**2.5. Antibacterial Analysis:**

Antibacterial activity of nanoparticles was assessed by measuring the values of zones of inhibition (ZOI) using agar wells diffusion <sup>39, 40</sup>. Wells of 5 mm were created in the nutrient medium. AgNPs solutions of 5, 10, 15, and 20 mg/mL were made using distilled water, and 25  $\mu$ L of each was added to wells. Distilled water was used as a control. The mean ZOI and standard deviations were evaluated <sup>41</sup>(Leelaprakash & Rose, 2011). The lowest dose of the nanoparticles needed to prevent bacterial growth was determined as the MIC <sup>42</sup>.

## 2.6. Statistical analysis:

Data were analyzed using Statistix10. analytical software. Experiment was replicated three time ( $r=3$ ). The results are shown as mean  $\pm$  standard deviation. Before analysis, all data were normalized with an arcsine transformation. The results are described as non-transformed means ( $\pm$ SEM). The differences between various groups were calculated by one-way analysis of variance (ANOVA) andf Tukey's test. A  $p \leq 0.05$  value was accepted as statistically significant.

## 3. Results

### 3.1. Green Synthesis of *Datura inoxia* AgNPs

The change of color from yellowish to brown inside the reaction vessels, specified the synthesis of AgNPs through the reduction of silver. The ideal temperature and pH for AgNPs were assessed to support labor- and time-efficient AgNP production in bulk. pH optimization was performed over a pH range of 2.0 to 9.0 and determined that a pH between 6.0 to 9.0 pH is ideal for AgNPs synthesis, indicating that moderately acidic to slightly alkaline conditions are the most effective. The optimal temperature was found to be between 10° and 100°C. The results showed that the ideal temperature range for green synthesis was between 70° and 90°C.

### 3.2. AgNPs Characterization

The UV-visible spectrophotometry showed taht  $\lambda_{\text{max}}$  for *Datura inoxia* AgNPs was recorded between 330-350 nm, with a maximum absorbance of 2.79, as shown in Fig. 1a. The X-ray diffraction (XRD) crystallographic analysis revealed that the AgNPs were polycrystalline, with the XRD spectrum covering  $2\theta$  values ranging from  $10^\circ$  to  $70^\circ$ . The prominent peaks for *Datura inoxia* were observed at  $33^\circ$ ,  $46^\circ$ , and  $58^\circ$ , corresponding to the (111), (200), and (220) planes, respectively. The XRD results are presented in Fig. 1b. SEM results revealed that the resulting nanoparticles were present in the form of clusters and had irregular shape (Fig. 2 a.). The image depicts polydispersity indicating that they vary in size, which is a common occurrence in green synthesis<sup>43, 44</sup>. As the nanoparticles are clusters, the Scherrer equation was used on X-ray diffraction data to determine the mean crystallite size having the size between 24 and 25nm. SEM results were confirmed by TEM Analysis which depicted that these clusters are made up of smaller units that are nearly spherical to slightly rod shaped (Fig. 2 b). Their size range between 20-30nm, that is close to the crystallite size (24-25nm) determined from XRD crystallography. Furthermore, the crystal structure is verified by HRTEM (Fig. 2 c, d). The results of FTIR analysis of this study show different stretches of bonds shown at different peaks ( $3231$ ,  $2913$ ,  $1604$ ,  $1345$ ,  $1313$ ,  $1045$ ,  $606$ , and  $485\text{ cm}^{-1}$ ) (Fig. 1 c).

**3.3. Antibacterial Assay**

Eight bacterial genera were isolated from six milk samples taken from Nili Ravi species of buffalo. These include 1) *Staphylococcus spp.*, 2) *Streptococcus spp.*, 3) *Escherichia coli*, 4) *Klebsiella spp.*, 5) *Pseudomonas aeruginosa*, 6) *Enterococcus spp.*, 7) *Enterobacter spp.*, and 8) *Corynebacterium spp.* The microorganisms were identified by morphological features and biochemical testing (e.g. simple staining, gram staining, motility test and catalase test). The antibacterial activity of *D. inoxia* AgNPs against the above genera, that cause bovine mastitis,

was determined using the diffusion method, as shown in Figure 3. The antibacterial activity was tested at concentrations of 5, 10, 15, and 20 mg/mL of *D. inoxia* AgNPs and control labeled as A, B, C, D, and E respectively on culturing plates. The bacterial inhibition zone was found to be proportional to the concentration of *D. inoxia* AgNPs. As the concentration of *D. inoxia* AgNPs increased, the bactericidal ability also increased, resulting in a larger diameter of the antibacterial ring as shown in Table 1. The study results showed that the maximum zone of inhibition was observed in group D (20 mg/mL of *D. inoxia* AgNPs) for *Staphylococcus spp.*, *Streptococcus spp.*, *Klebsiella spp.*, *Enterococcus spp.*, *Enterobacter spp.*, and *Corynebacterium spp.* While, group C (15 mg/mL of *D. inoxia* AgNPs) exhibited the highest zone of inhibition for *Escherichia coli*, *Klebsiella spp.*, and *Pseudomonas spp.* Moreover, the maximum antibacterial activity of AgNPs was observed at a minimum inhibitory concentration (MIC) of 10  $\mu$ L, particularly against *Staphylococcus* species presented in Fig 4.

**Table 1:** Tabular display of antibacterial activity by *D. inoxia* AgNPs as ZOI (mm)

Sr.	Bacterial Genera	Zone of Inhibition (mm)				
		5 mg/mL	10 mg/mL	15 mg/mL	20 mg/mL	Control
1	<i>Staphylococcus spp.</i>	9.1 $\pm$ 0.4 <sup>c</sup>	10.2 $\pm$ 0.6 <sup>c</sup>	15.1 $\pm$ 0.3 <sup>b</sup>	18.3 $\pm$ 0.2 <sup>a</sup>	00 $\pm$ 00 <sup>d</sup>
2	<i>Streptococcus spp.</i>	8.4 $\pm$ 0.2 <sup>c</sup>	9.1 $\pm$ 0.5 <sup>c</sup>	10.4 $\pm$ 0.4 <sup>b</sup>	11.1 $\pm$ 0.3 <sup>a</sup>	00 $\pm$ 00 <sup>d</sup>
3	<i>Escherichia coli</i>	8.3 $\pm$ 0.3 <sup>c</sup>	9.7 $\pm$ 0.1 <sup>c</sup>	11.4 $\pm$ 0.7 <sup>a</sup>	10.2 $\pm$ 0.4 <sup>b</sup>	00 $\pm$ 00 <sup>d</sup>
4	<i>Klebsiella spp.</i>	7.1 $\pm$ 0.3 <sup>c</sup>	9.0 $\pm$ 0.4 <sup>b</sup>	10.1 $\pm$ 0.2 <sup>a</sup>	10.2 $\pm$ 0.6 <sup>a</sup>	00 $\pm$ 00 <sup>d</sup>
5	<i>Pseudomonas spp.</i>	7.9 $\pm$ 0.7 <sup>c</sup>	8.1 $\pm$ 0.4 <sup>c</sup>	11.8 $\pm$ 0.2 <sup>a</sup>	10.4 $\pm$ 0.1 <sup>b</sup>	00 $\pm$ 00 <sup>d</sup>
6	<i>Enterococcus spp.</i>	8.8 $\pm$ 0.2 <sup>c</sup>	8.9 $\pm$ 0.6 <sup>c</sup>	10.2 $\pm$ 1.1 <sup>b</sup>	15.5 $\pm$ 0.3 <sup>a</sup>	00 $\pm$ 00 <sup>d</sup>
7	<i>Enterobacter spp.</i>	8.1 $\pm$ 0.4 <sup>c</sup>	11.6 $\pm$ 0.8 <sup>b</sup>	10.4 $\pm$ 0.2 <sup>b</sup>	14.1 $\pm$ 0.2 <sup>a</sup>	00 $\pm$ 00 <sup>d</sup>
8	<i>Corynebacterium spp.</i>	7.2 $\pm$ 0.5 <sup>c</sup>	8.7 $\pm$ 0.1 <sup>c</sup>	9.8 $\pm$ 0.2 <sup>b</sup>	11.2 $\pm$ 0.6 <sup>a</sup>	00 $\pm$ 00 <sup>d</sup>

4. Discussion

A green synthesis technique was employed to produce AgNPs using *Datura innoxia* leaf extract, which act as both reducing and stabilizing agent. The phytochemical present in the extract like flavonoids, phenolic acids, alkaloids, glycosides and saponins jointly acts as effective bio reducer and capping agent, facilitating the formation of stable AGNPs during the green synthesis <sup>25, 27</sup>. The appearance of a yellowish-brown color in reaction mixture indicated successful nanoparticle synthesis, consistent with observation reported by <sup>45</sup>, and further characterized using UV-Vis spectroscopy, XRD, SEM, FTIR, TEM and HR-TEM microscopy analysis. The observed surface plasmon resonance peak between 330-350 nm and crystalline size range of 24-25 are aligned with previous studies <sup>26, 46</sup> where AgNPs were synthesized from *D. stramonium* leaves and *D. innoxia* flowers <sup>47-49</sup>. The magnitude, peak wavelength, and spectral width of a nanoparticle depends on its size, shape, and composition. According to previous studies, the UV-visible absorbance spectrum is influenced by the aggregation state of the nanoparticles <sup>50</sup>. A variety of phytoconstituents found in the leaf extract may be responsible for the reduction of metal ions <sup>51</sup>. The broad peak at 3231 cm<sup>-1</sup>, indicates the presence of hydroxyl (-OH) groups (most likely from polyphenols, flavonoids, or water molecules) and amine or amide groups from the *D. innoxia* extract <sup>51</sup>. The C-H stretching (alkane groups) vibrations found in lipids, proteins, or organic compounds produced from plants are represented by the peak at 2913 cm<sup>-1</sup>. The peak at 1604 cm<sup>-1</sup> indicates the presence of carbonyl (C=O) functional groups from carboxylic acids, flavonoids, or C=C stretching from aromatic chemicals in plant extracts <sup>46</sup>. The peaks at 1345 cm<sup>-1</sup> and 1313 cm<sup>-1</sup>—C-N stretching or C-H bending, respectively indicate the presence of amines from proteins or phenolic chemicals. Alcohols, ethers, esters, or

polysaccharides may be the cause of the absorption peak at  $1045\text{ cm}^{-1}$ . The vibrations at  $1045\text{ cm}^{-1}$  may be the cause of organo-phosphorous <sup>51</sup>.

SEM results showed that the nanoparticles were in the form of clusters and had irregular shape, was confirmed by TEM analysis which depicted that these clusters are made up of smaller units (20-30nm) that are nearly spherical to slightly rod shaped are aligned with previous studies on AgNPs from *D. stramonium* leaves extract showed that in SEM imaging, clumping and formation of nano-sized structures were visible, while TEM analysis, showed spherical nanoparticles with a size of less than 30 nm was seen <sup>52</sup>. The narrow peaks in the XRD spectrum indicate a higher crystallinity of the synthesized nanoparticles which are confirmed by HR-TEM. This crystalline structure of the synthesized nanoparticles significantly influences toxicity, as a higher degree of crystallinity correlates with more predictable biological activity. For example, the interaction of nanoparticles with bacterial cells becomes more uniform, enhancing the release of metal ions <sup>53</sup>.

The synthesized AgNPs showed concentration dependent antibacterial activity against both gram positive and gram negative bacteria. The highest zone of inhibition ( $18.3\pm0.2$ ) was recorded at concentration 20 mg/mL, against *Staphylococcus spp.* These findings are consistent with studies that report higher susceptibility of *Staphylococcus aureus* to AgNPs derived from other plant extract <sup>45, 54</sup>. *Enterococcus spp.*, *Enterobacter spp.*, also showed significant sensitivity, while *Escherichia coli* and *Pseudomonas spp.* Displayed comparatively lower inhibition zones. This variation may relate to cell wall difference of gram positive and gram negative bacteria. Compared with earlier research, the antimicrobial effects observed here align with those using AgNPs synthesized from other medicinal plants such as *Azadirachta indica* <sup>10</sup>, *Ocimum tenuiflorum* <sup>55</sup>, and *Datura metel* <sup>5</sup>, suggesting that *D. inoxia* is a similarly effective

reducing agent for AgNPs with comparable antibacterial properties. Unlike some studies that used higher AgNP concentrations (50–200 µg/mL) <sup>56, 57</sup>, the present study achieved notable activity at lower concentrations (5–20 mg/mL), with lower MIC of AgNPs between range of 10-25 µL for bacterial strains test.

**5. Conclusion**

Biosynthesized *D. inoxia* silver nanoparticles (AgNPs) exhibit significant antibacterial activity against multiple mastitis causing bacterial genera, particularly gram positive strains. While the results support their potential as an alternative antimicrobial approach, further research including in vivo trials, toxicity assessments, and long-term stability analysis is essential before clinical or field application can be recommended.

**6. Statements and Declarations**

**6.1. Ethical statement :**The study was approved by Ethical Committee of University of Education Lahore, Pakistan, for the use of animals.

**6.2. Data Availability Statement:** The data that support the findings of this study are available from the corresponding author upon reasonable request.

**6.3. Funding Statement:** Nill

**Authors contribution:** S. Qadeer and F. Bibi designed the study, executed the experiment and drafted the manuscript. M. Asad and A. Ashraf provided expertise in practical work, data analysis and drafting of manuscript.

**Conflicts of Interest:** The authors declare no conflicts of interest.

**References**

1. Yusuf B, Abraha B, Salih K, et al. In vitro antibacterial evaluation of four selected medicinal plants against *Staphylococcus aureus* isolated from bovine mastitis in Mieso District West Hararghe Zone, Oromia Regional State, Ethiopia. *The Open Microbiology Journal* 2022; 16.

2. Sharun K, Dhama K, Tiwari R, et al. Advances in therapeutic and managemental approaches of bovine mastitis: a comprehensive review. *Veterinary Quarterly* 2021; 41: 107-136.

3. Dabele DT, Borena BM, Admasu P, et al. Prevalence and risk factors of mastitis and isolation, identification and antibiogram of staphylococcus species from mastitis positive zebu cows in toke kutaye, cheliya, and dendi districts, west shewa zone, Oromia, Ethiopia. *Infection and Drug Resistance* 2021; 987-998.
4. Ashraf A and Imran MJAhrr. Causes, types, etiological agents, prevalence, diagnosis, treatment, prevention, effects on human health and future aspects of bovine mastitis. *Animal health research reviews* 2020; 21: 36-49.
5. Vo-Van Q-B, Duong TH and Le TKAJJoCEA. Biosynthesis of silver nanoparticles using curcumin against the bovine mastitis bacteria. *Journal of Central European Agriculture* 2023; 24: 505-512.
6. Al-Dujaily AH and Mahmood AK. The effectiveness of biogenic silver nanoparticles in the treatment of caprine mastitis induced by Staphylococcus aureus. *Iraqi Journal of Veterinary Sciences* 2021.
7. Bhaviripudi S, Mile E, Steiner SA, et al. CVD synthesis of single-walled carbon nanotubes from gold nanoparticle catalysts. *Journal of the American Chemical Society* 2007; 129: 1516-1517.
8. Bar H, Bhui DK, Sahoo GP, et al. Green synthesis of silver nanoparticles using latex of Jatropha curcas. *Colloids and surfaces A: Physicochemical and engineering aspects* 2009; 339: 134-139.
9. Larue C, Castillo-Michel H, Sobanska S, et al. Foliar exposure of the crop Lactuca sativa to silver nanoparticles: evidence for internalization and changes in Ag speciation. *Journal of hazardous materials* 2014; 264: 98-106.
10. Alqahtani O, Mirajkar KK, Kumar K R A, et al. In vitro antibacterial activity of green synthesized silver nanoparticles using Azadirachta indica aqueous leaf extract against MDR Pathogens. *Molecules* 2022; 27: 7244.
11. Beyth N, Hourri-Haddad Y, Domb A, et al. Alternative antimicrobial approach: nano-antimicrobial materials. *Evidence-Based Complementary and Alternative Medicine* 2015; 2015: 246012.
12. Mohammed HA, Amin MA, Zayed G, et al. In vitro and in vivo synergistic wound healing and anti-methicillin-resistant Staphylococcus aureus (MRSA) evaluation of liquorice-decorated silver nanoparticles. *The Journal of Antibiotics* 2023; 76: 291-300.
13. Ashij MA, Al-Shmgani HS, Sulaiman GM, et al. Investigation of antibacterial activity and wound healing promotion properties induced by bromelain-loaded silver nanoparticles. *Plasmonics* 2024; 19: 1903-1916.
14. Nagy A, Harrison A, Sabbani S, et al. Silver nanoparticles embedded in zeolite membranes: release of silver ions and mechanism of antibacterial action. *International journal of nanomedicine* 2011; 1833-1852.
15. Gurunathan S, Han JW, Dayem AA, et al. Oxidative stress-mediated antibacterial activity of graphene oxide and reduced graphene oxide in Pseudomonas aeruginosa. *International journal of nanomedicine* 2012; 5901-5914.
16. Leung YH, Ng AM, Xu X, et al. Mechanisms of antibacterial activity of MgO: non-ROS mediated toxicity of MgO nanoparticles towards Escherichia coli. *Small* 2014; 10: 1171-1183.
17. Prathna T, Chandrasekaran N, Raichur AM, et al. Kinetic evolution studies of silver nanoparticles in a bio-based green synthesis process. *Physicochemical and Engineering Aspects* 2011; 377: 212-216.
18. Hussein NN, Al-Azawi K, Sulaiman GM, et al. Silver-cored Ziziphus spina-christi extract-loaded antimicrobial nanosuspension: overcoming multidrug resistance. *Nanomedicine* 2023; 18: 1839-1854.
19. Angelina EDR, Bavyaa R and Rajagopal RJJSRP. Green synthesis and characterization of silver nanoparticles using Fenugreek seed extract. *Int J Sci Res Pub* 2013; 3: 1-3.
20. Satyavani K, Ramanathan T and Gurudeeban SJDJNB. Green synthesis of silver nanoparticles by using stem derived callus extract of bitter apple (Citrullus colocynthis). *Dig J Nanomater Biostruct* 2011; 6: 1019-1024.

1  
2  
3  
4  
5  
6  
7  
8  
9  
10  
11  
12  
13  
14  
15  
16  
17  
18  
19  
20  
21  
22  
23  
24  
25  
26  
27  
28  
29  
30  
31  
32  
33  
34  
35  
36  
37  
38  
39  
40  
41  
42  
43  
44  
45  
46  
47  
48  
49  
50  
51  
52  
53  
54  
55  
56  
57  
58  
59  
60

21. Saman S, Chen C-C, Malak N, et al. Ethanolic extracts of *Datura innoxia* have promising acaricidal activity against *Rhipicephalus microplus* as it blocks the glutathione s-transferase activity of the target tick. *Genes* 2022; 14: 118.

22. Ramadan MF, Zayed R and El-Shamy HJFC. Screening of bioactive lipids and radical scavenging potential of some solanaceae plants. *Food Chemistry* 2007; 103: 885-890.

23. Shama AI, Abd-Kreem Y, Fadowa A, et al. In vitro antibacterial and antifungal activity and *Datura innoxia* extracts. *International Journal of Environment* 2014; 3: 173-185.

24. Al-Zharani M, Nasr FA, Alqahtani AS, et al. In vitro cytotoxic evaluation and apoptotic effects of *Datura innoxia* grown in Saudi Arabia and phytochemical analysis. *Applied Sciences* 2021; 11: 2864.

25. Chamani E, Ebrahimi R, Khorsandi K, et al. In vitro cytotoxicity of polyphenols from *Datura innoxia* aqueous leaf-extract on human leukemia K562 cells: DNA and nuclear proteins as targets. *Drug and Chemical Toxicology* 2020; 43: 138-148.

26. Gajendran B, Durai P, Varier KM, et al. Green synthesis of silver nanoparticle from *Datura innoxia* flower extract and its cytotoxic activity. *BioNanoScience* 2019; 9: 564-572.

27. Ayuba V, Ojobe T and Ayuba SJJMPR. Phytochemical and proximate composition of *Datura innoxia* leaf, seed, stem, pod and root. *J Med Plants Res* 2011; 5: 2952-2955.

28. Manach C, Williamson G, Morand C, et al. Bioavailability and bioefficacy of polyphenols in humans. I. Review of 97 bioavailability studies. *The American journal of clinical nutrition* 2005; 81: 230S-242S.

29. Asif M, Yasmin R, Asif R, et al. Green synthesis of silver nanoparticles (AgNPs), structural characterization, and their antibacterial potential. *Dose-Response* 2022; 20: 15593258221088709.

30. Okafor F, Janen A, Kukhtareva T, et al. Green synthesis of silver nanoparticles, their characterization, application and antibacterial activity. *International journal of environmental research and public health* 2013; 10: 5221-5238.

31. Forough M and Farhadi KJTJEES. Biological and green synthesis of silver nanoparticles. *Turkish J Eng Env Sci* 2010; 34: 281-287.

32. Filippi MCC, Da Silva GB, Silva-Lobo VL, et al. Leaf blast (*Magnaporthe oryzae*) suppression and growth promotion by rhizobacteria on aerobic rice in Brazil. *Biological control* 2011; 58: 160-166.

33. Katz DSJML. The streak plate protocol. *Microbe Library* 2008: 1-14.

34. Tankeshwar AJMORD. Streak plate method: Principle, procedure, uses. *Microbe Online Retrieved December* 2022; 12: 2022.

35. Ding K, Luo Y, Sun T, et al. Bioremediation of soil contaminated with petroleum using forced-aeration composting. *Pedosphere* 2002; 12: 145-150.

36. Huang T-L and Ren L. Simulating and modeling of the runoff pollution of petroleum pollutants in loess plateau. *China Environmental Science* 2000.

37. Wu T and Crapper MJD. A computational fluid dynamics based model of the ex-situ remediation of hydrocarbon contaminated soils. *Desalination* 2009; 248: 262-270.

38. Khan JA and Rizvi SHAJAiasr. Isolation and characterization of micro-organism from oil contaminated sites. *Advances in applied science researc* 2011; 2: 455-460.

39. Shahzada S, Shireen F and Fida SJAJOPR. Biological evaluation of efficacy of *Aloe barbadensis* L. extract. *American Journal Of Pharm Research* 2013; 3.

40. Qais FA, Khan MS and Ahmad IJMp. Broad-spectrum quorum sensing and biofilm inhibition by green tea against gram-negative pathogenic bacteria: Deciphering the role of phytocompounds through molecular modelling. *Microbial pathogenesis* 2019; 126: 379-392.

41. Leelaprakash G and Rose JCJP. In vitro antimicrobial and antioxidant activity of *Momordica charantia* leaves. *Pharmacophore* 2011; 2: 207-215.

42. Tripathi K. *Essentials of medical pharmacology*. Jaypee Brothers medical publishers, 2018.

43. Ahmed S, Ahmad M, Swami BL, et al. Green synthesis of silver nanoparticles using *Azadirachta indica* aqueous leaf extract. *Journal of radiation research and applied sciences* 2016; 9: 1-7.
44. Sharma NK, Vishwakarma J, Rai S, et al. Green route synthesis and characterization techniques of silver nanoparticles and their biological adeptness. *ACS omega* 2022; 7: 27004-27020.
45. Kaur J, Gupta N, Kaur M, et al. Antibacterial Effects of Green Synthesized AgNPs from *datura* metel leaf extracts. *Int J Pure Appl Biosci* 2019; 7: 247-252.
46. Gomathi M, Rajkumar P, Prakasam A, et al. Green synthesis of silver nanoparticles using *Datura stramonium* leaf extract and assessment of their antibacterial activity. *Resource-Efficient Technologies* 2017; 3: 280-284.
47. Vidhu V, Aromal SA, Philip DJSAPAM, et al. Green synthesis of silver nanoparticles using *Macrotyloma uniflorum*. *Molecular and Biomolecular Spectroscopy* 2011; 83: 392-397.
48. Wypij M, Jędrzejewski T, Trzcińska-Wencel J, et al. Green synthesized silver nanoparticles: antibacterial and anticancer activities, biocompatibility, and analyses of surface-attached proteins. *Frontiers in microbiology* 2021; 12: 632505.
49. Devaraj P, Kumari P, Aarti C, et al. Synthesis and characterization of silver nanoparticles using cannonball leaves and their cytotoxic activity against MCF-7 cell line. *Journal of nanotechnology* 2013; 2013: 598328.
50. George G, Wilson R and Joy J. Ultraviolet spectroscopy: a facile approach for the characterization of nanomaterials. *Spectroscopic methods for nanomaterials characterization* Elsevier, 2017, pp.55-72.
51. Sundareswari C and Sudarmani DJE. Synthesis and characterization of silver nanoparticles using *Datura metel* L.(Solanaceae) leaf extract and its larvicidal activity on *Epilachna vigintioctopunctata* F. *Entomon* 2023; 48: 519-524.
52. Chandan G, Pal S, Kashyap S, et al. Synthesis, characterization and anticancer activities of silver nanoparticles from the leaves of *Datura stramonium* L. *Nanofabrication* 2021; 6: 25-35.
53. Abbasi R, Shineh G, Mobaraki M, et al. Structural parameters of nanoparticles affecting their toxicity for biomedical applications: a review. *Journal of Nanoparticle Research*, 2023; 25: 43.
54. Ruparelia JP, Chatterjee AK, Duttagupta SP, et al. Strain specificity in antimicrobial activity of silver and copper nanoparticles. *Acta biomaterialia* 2008; 4: 707-716.
55. Patil RS, Kokate MR, Kolekar SSJSAPAM, et al. Bioinspired synthesis of highly stabilized silver nanoparticles using *Ocimum tenuiflorum* leaf extract and their antibacterial activity. *Molecular and Biomolecular Spectroscopy* 2012; 91: 234-238.
56. Ojha AK, Rout J, Behera S, et al. Green synthesis and characterization of zero valent silver nanoparticles from the leaf extract of *Datura metel*. *Int J Pharm Res Allied Sci* 2013; 2: 31-35.
57. Logeswari P, Silambarasan S and Abraham JJJoSCS. Synthesis of silver nanoparticles using plants extract and analysis of their antimicrobial property. *Journal of Saudi Chemical Society*, 2015; 19: 311-317.

## Figure caption

**Fig. 1.** UV (a), XRD (b) micrographs of *D. inoxia* AgNPs, (c) FTIR micrograph of *D. inoxia* AgNPs

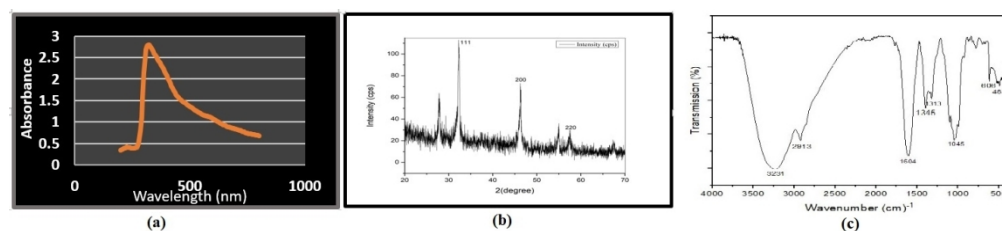
**Fig. 2:** Characterization of *D. inoxia* AgNPs (a) SEM, (b) TEM, (c, d) HR-TEM

1  
2  
3  
4  
5  
6  
7  
8  
9  
10  
11  
12  
13  
14  
15  
16  
17  
18  
19  
20  
21  
22  
23  
24  
25  
26  
27  
28  
29  
30  
31  
32  
33  
34  
35  
36  
37  
38  
39  
40  
41  
42  
43  
44  
45  
46  
47  
48  
49  
50  
51  
52  
53  
54  
55  
56  
57  
58  
59  
60

**Fig. 3.** (ZOI); a) *Staphylococcus spp.*, b) *Streptococcus spp.*, c) *Escherichia coli*, d) *Klebsiella spp.*, e) *Pseudomonas aeruginosa*, f) *Enterococcus spp.*, g) *Enterobacter spp.*, and h) *Corynebacterium spp.*

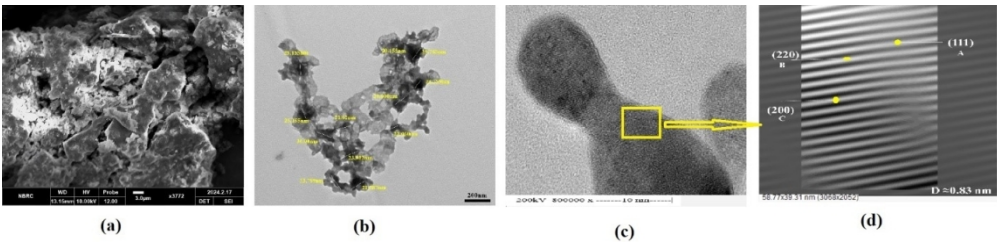
**Figure 4.** MIC of *D. anoxia* AgNPs and error bar shows standard error of mean (n=3).

For Peer Review



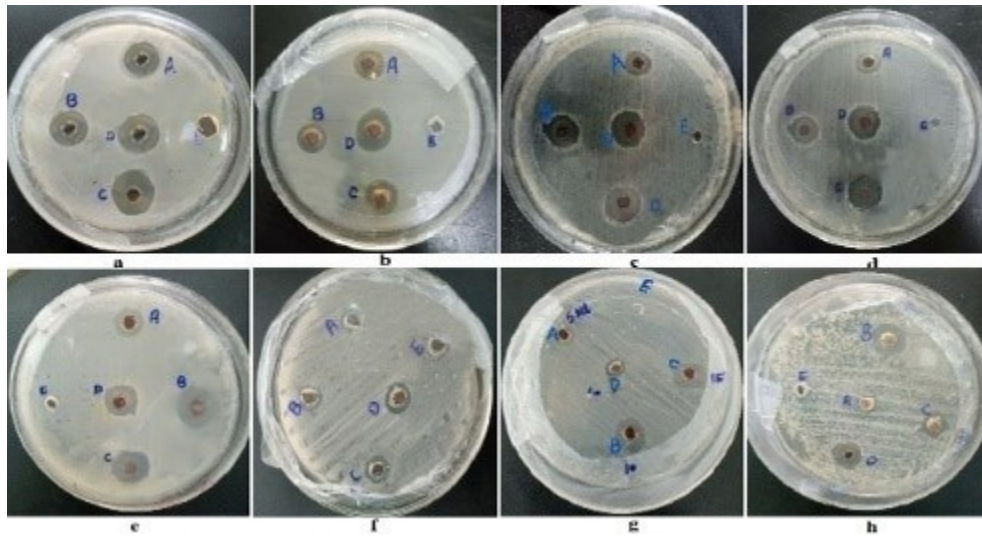
UV (a), XRD (b) micrographs of *D. inoxia* AgNPs, (c) FTIR micrograph of *D. inoxia* AgNPs

258x58mm (144 x 144 DPI)



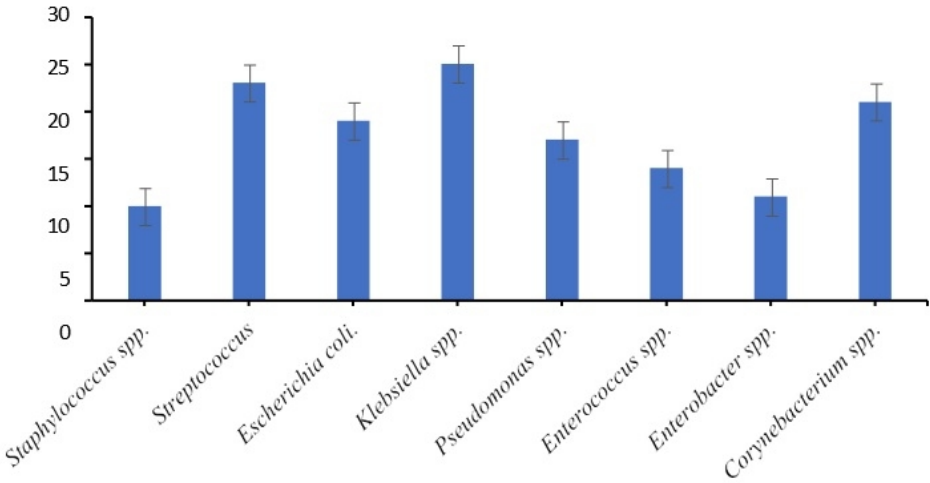
Characterization of *D. inoxia* AgNPs (a) SEM, (b) TEM, (c, d) HR-TEM

165x39mm (220 x 220 DPI)



(ZOI); a) *Staphylococcus* spp., b) *Streptococcus* spp., c) *Escherichia coli*, d) *Klebsiella* spp., e) *Pseudomonas aeruginosa*, f) *Enterococcus* spp., g) *Enterobacter* spp., and h) *Corynebacterium* spp.

130x69mm (96 x 96 DPI)



MIC of *D. anoxia* AgNPs and error bar shows standard error of mean (n=3).

132x67mm (144 x 144 DPI)